

Synthesis and characterization of $\text{Cu}_2\text{ZnSnS}_4$ nanocrystals prepared by microwave irradiation method

Yu Zhao¹ · Wanku Tao¹ · Xu Chen¹ · Jun Liu¹ · Aixiang Wei¹

Received: 8 February 2015 / Accepted: 22 April 2015 / Published online: 29 April 2015
© Springer Science+Business Media New York 2015

Abstract In this study, we report a rapid and single-step synthesis of $\text{Cu}_2\text{ZnSnS}_4$ (CZTS) nanocrystals using microwave-assisted solution method. The influence of reaction temperature and reaction time on the phase purity, crystallographic structure, morphology and optical property of CZTS particles were investigated using X-ray diffraction, Raman spectroscopy, scanning electronic microscope, transmission electron microscopy and ultraviolet–visible spectrometer. Results revealed that the single kesterite CZTS particles with no secondary phase can be obtained by preparing samples at minimal temperature of 170 °C. The sphere-like particles, each of which contains many nanocrystals, decrease effectively in size when increasing the reaction temperature from 170 to 200 °C. The CZTS nanocrystals have an optical band gap around 1.5 eV, which is optimal for photovoltaic applications. In addition, minimal reaction time of 10 min is also essential for the growth of single kesterite CZTS. Our study demonstrated that appropriate reaction temperature and reaction time are crucial for the synthesis of high-quality CZTS by microwave irradiation method.

1 Introduction

The $\text{CuIn}_x\text{Ga}_{1-x}\text{S}(\text{Se})_2$ (CIGS) thin film solar cell has attracted great interest due to its high power conversion efficiency and stability [1, 2]. However, indium and gallium are rare and expensive elements, which increase the production costs and hinder the development of CIGS thin film solar cells. For years, scientists are stimulated to find an alternative In- and Ga-free solar absorbers composed of abundant, inexpensive, and nontoxic elements. CZTS has been considered as the most promising photon absorber materials to substitute CIGS [3]. CZTS, which is structural analogue to CIGS, has optimum direct band gap energy of 1.5 eV and a relatively large absorption coefficient (10^4 cm^{-1}) [4]. Recently, it has been reported that a non-vacuum deposition route led to a record of 11.2 % [5] power conversion efficiency for CZTS-based thin film solar cells, while theoretically predicted efficiency for CZTS-based solar cells was calculated to be as high as 32.2 % [6]. Therefore, a great amount of work has to be done in order to bring the power conversion efficiency closer to the theoretical limit. Various vacuum deposition methods such as sputtering [7], pulsed laser deposition [8] and chemical vapour deposition [9] have been adapted to the fabrication of CZTS thin film. Solution-based synthesis of CZTS offers a low cost and high throughput alternative to vacuum-based methods. Several solution-based approaches to synthesize CZTS have been studied, for example, the spray pyrolysis [10], the sol–gel method [11, 12], microwave-assisted solution methods [13–16], hot-injection solution synthesis method [17], and solvothermal method [18, 19]. Microwave irradiation is an emerging versatile technique for the controlled synthesis of various nanomaterials due to its advantages like favourable homogeneity, shorter crystallization time, better size control, improved yield, good

✉ Aixiang Wei
weiax@gdut.edu.cn

¹ Guangdong Provincial Key Laboratory of Functional Soft Condensed Matter, School of Material and Energy, Guangdong University of Technology, Guangzhou 510006, China

purity and reproducibility. Recently, there are several reports about the preparation of CZTS particles by microwave irradiation [13–16, 20–24]. In general, the CZTS films used as the absorbers of thin film solar cell can be obtained by printing, spraying, or dip-coating the CZTS particles onto larger area substrates [25]. The influence of synthesis conditions on the properties of CZTS particles has been investigated previously. Shin et al. [21] reported the critical effect of Cu concentrations on the synthesis of single phase CZTS nanocrystals. Wang et al. [22] reported the effects of sulfur sources on the morphology and size of the CZTS nanoparticles. Chen et al. [23] and Wang et al. [24] studied the influences of the reaction temperature on the chemical composition and phase purity of CZTS nanocrystals. Nevertheless, a further study and understanding of the microwave assisted synthesis of CZTS particles is necessary for the research community.

Hence, in this paper, we report a facile, single-step synthesis of CZTS nanocrystals by microwave-assisted solution method. The influence of reaction temperature and reaction time on the phase purity, crystallographic structure, morphology and optical property of CZTS nanocrystals were investigated in detail respectively.

2 Experimental details

All the chemicals used in the present work are of analytical grade and used without further purification. The CZTS nanocrystals were prepared by microwave-assisted solution method. A typical synthesis process is as follows: 0.004 mmol of copper(II) chloride dihydrate ($\text{CuCl}_2 \cdot 2\text{H}_2\text{O}$), 0.008 mmol of zinc(II) chloride dihydrate ($\text{ZnCl}_2 \cdot 2\text{H}_2\text{O}$), 0.002 mmol of tin(II) chloride dihydrate ($\text{SnCl}_2 \cdot 2\text{H}_2\text{O}$) and 0.010 mmol of thiourea ($\text{CH}_4\text{N}_2\text{S}$) were dissolved, mixed and stirred in 80 ml of ethylene glycol as the precursor solution. In the process, it can be seen that the colors of solution change from green to colorless. The precursor solution was added to a flask, and subsequently placed in a 2.45 GHz XianHu XH-100A microwave reactor operated at 800 W for 20 min. Thereafter, the microwave power was turned off and the sample was cooled down to room temperature by air flow. After the reaction, the precipitate was washed several times with ethanol. The black precipitates at the bottom of the flask were dried in a vacuum at 60 °C. Finally, the as-prepared CZTS nanocrystals were obtained without any post-treatment. In order to study the effect of reaction temperature and reaction time on the properties of the CZTS nanocrystals, two series of samples were prepared by varying the reaction temperature or the reaction time separately while keeping the other reagent concentrations constant. Note that the boiling point of ethylene glycol is 197.3 °C,

therefore we conducted our experiment at temperature no higher than 200 °C. The deposition parameters for different samples are listed in Table 1.

The crystallographic structure and phase purity of the as-prepared CZTS particles were investigated using X-ray diffraction (XRD, D/MAXUltimaIV, Rigaku) with Cu-K α radiation ($\lambda = 0.1542$ nm), micro-Raman spectroscopy (Renishaw, 514.5 nm) and high resolution transmission electron microscopy (HRTEM, JEM2010-HR). The morphology of the CZTS particles was analyzed using scanning electron microscopy (SEM, S-3400N, Hitachi). Absorption spectra were recorded using ultraviolet–visible spectrometer (T6).

3 Results and discussion

3.1 Effect of reaction temperature on property of CZTS nanocrystals

3.1.1 Structure analysis of CZTS nanocrystals

The XRD patterns of CZTS particles prepared at different reaction temperature were shown in Fig. 1. At reaction temperature of 160 °C and above, the major XRD diffraction peaks appeared at 28.40°, 47.42° and 56.10°, can be indexed (112), (220) and (312) planes of the kesterite crystal structure (JCPDS No. 26-0575), which is in good agreement with the reported profile of stoichiometric CZTS with kesterite structure with cell parameters $a = b = 0.5427$ nm, $c = 1.0848$ nm [19]. No obvious peaks resulting from impurities were observed for samples prepared at temperature higher than 160 °C. However, for sample prepared at 140 °C, its diffraction peaks appeared at $2\theta = 26.88^\circ$, 30.08° , 34.56° and 35.70° could be attributed to the binary sulfide phases of ZnS, SnS, $\text{Cu}_{31}\text{S}_{16}$ and Cu_{2-x}S . When temperature increases to 150 °C, the intensity of the diffraction peaks originated from binary sulfide decreases, while the diffraction peaks around 28.40°, which can be indexed (112) of the kesterite CZTS, becomes sharper.

XRD is generally used as the main tool to analyze the structure of such compounds, but it is not sufficient to identify most of the minor phases, since cubic ZnS (JCPDS No. 5-0566) and tetragonal Cu_2SnS_3 (JCPDS No. 89-4714) have very similar diffraction pattern with tetragonal CZTS. Hence, Raman spectroscopy was used to further confirm the phase purity of as-synthesized samples. Figure 2 shows the Raman spectra for CZTS particles synthesized at different reaction temperature. The Raman spectrum of CZTS particles synthesized at 160 °C and above exhibits intense peak at 289 and 331 cm^{-1} (on average), which can be attributed to the kesterite structure CZTS [26]. The

Table 1 Parameters of deposition process for various samples

Sample Nos.	Reaction solutions (mmol)				Solvent (CH ₂ OH) ₂ (ml)	Reaction parameters		
	CuCl ₂ ·2H ₂ O	ZnCl ₂ ·2H ₂ O	SnCl ₂ ·2H ₂ O	CS (NH ₂) ₂		Temperature (°C)	Power (W)	Time (min)
A1	0.004	0.008	0.002	0.010	80	140	800	20
A2	0.004	0.008	0.002	0.010	80	150	800	20
A3	0.004	0.008	0.002	0.010	80	160	800	20
A4	0.004	0.008	0.002	0.010	80	170	800	20
A5	0.004	0.008	0.002	0.010	80	180	800	20
A6	0.004	0.008	0.002	0.010	80	190	800	20
A7	0.004	0.008	0.002	0.010	80	200	800	20
B1	0.004	0.008	0.002	0.010	80	180	800	5
B2	0.004	0.008	0.002	0.010	80	180	800	10
B3	0.004	0.008	0.002	0.010	80	180	800	15
B4	0.004	0.008	0.002	0.010	80	180	800	20

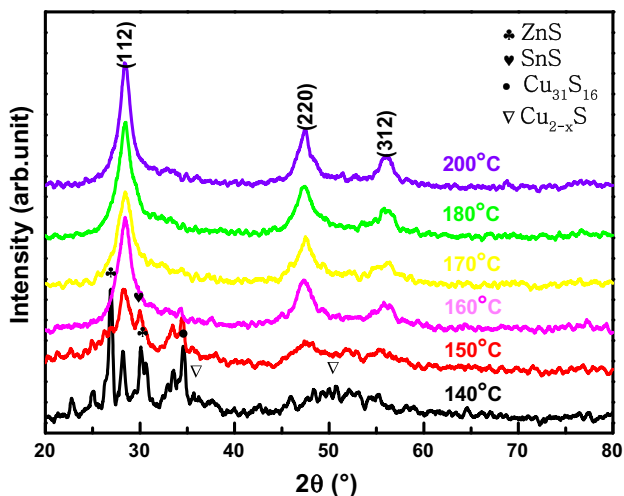


Fig. 1 X-ray diffraction patterns of the CZTS nanocrystals prepared at different reaction temperature. Reaction time of all the samples was fixed to 20 min

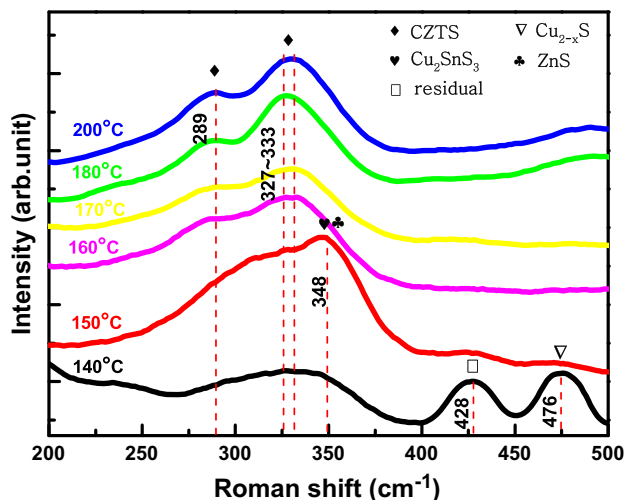


Fig. 2 Raman spectra of the CZTS nanocrystals prepared at different reaction temperature. Reaction time of all the samples was fixed to 20 min

characteristic Raman peaks of 331 cm⁻¹ arise from A₁ vibration mode of lattice, where the group VI atoms (S) vibrate while the rest of atoms (Cu, Zn and Sn) remain fixed. Raman peak of 331 cm⁻¹ is red shifted compared to bulk CZTS (336 cm⁻¹) due to a decrease in phonon frequency for the A₁ vibrational mode associated with particle size [27]. We have noticed that such red-shift phenomena can be found in many of the other reports of CZTS particle prepared by microwave irradiation method, such as Refs. [13, 24, 28]. No other obvious characteristic peaks of impurity phases, such as Cu₂SnS₃, Cu₃SnS₄, Cu_{2-x}S and ZnS, were observed. Those results confirm that the particles synthesized at 160 °C and above are purely CZTS phases. Samples synthesized at 140 and 150 °C exhibit no obvious

characteristic Raman peaks of the kesterite structure CZTS. For sample synthesized at 140 °C, the broad peak centered at around 333 cm⁻¹ can be considered as the superimposed spectrums of tetragonal CZTS (289 and 339 cm⁻¹ [26]), tetragonal Cu₂SnS₃ (297 and 352 cm⁻¹ [26]) and cubic ZnS (352 cm⁻¹ [26]). The peak at 476 cm⁻¹ can be assigned to Cu_{2-x}S (475 cm⁻¹ [26]). The origin of peak at 428 cm⁻¹ is not clear since close Raman peak of CZTS related material has not been found in literature. However, such Raman peak is possibly related to residual complex due to the incomplete reaction of precursor. The peak at 348 cm⁻¹ for the sample synthesized at 150 °C can be assigned to Cu₃SnS₄ (348 cm⁻¹ [26]) or tetragonal Cu₂SnS₃ (352 cm⁻¹ [26]) or cubic ZnS (352 cm⁻¹ [26]) or mixture of them.

Crystallographic structure of the CZTS particles (sample A5) has been analyzed using HRTEM. The HRTEM image in Fig. 3b shows that the lattice spacing of 0.32 nm corresponds to the (112) plane of the kesterite structure CZTS. The results of XRD, Raman and HRTEM all confirmed that those particles are CZTS in kesterite quaternary structure.

The characterizations of the CZTS synthesized at different reaction temperature demonstrated that temperature is a crucial factor for the growth of high-quality CZTS particles. Higher synthesis temperature will convert the sulfide into CZTS and lead to the growth of CZTS with high phase purity. On the contrary, particles synthesized at lower temperature are a mixture of CZTS, binary and ternary sulfide. The analysis of XRD patterns and Raman spectra indicated that the single phase kesterite CZTS particles can only be obtained when the reaction temperature is 160 °C and above. This result is in good agreement with the previously reported temperature of 160 °C [16] and 190 °C [28] for the synthesis of kesterite CZTS using microwave irradiation method.

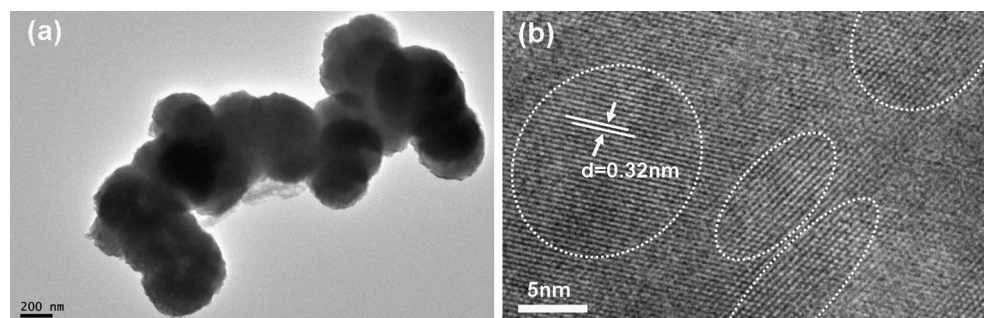
The average crystallite sizes calculated using well-known Debye–Scherrer equation based on the (112) peaks of XRD patterns are 4.94, 4.97, 4.97 and 6.47 nm for samples prepared at temperature of 160, 170, 180, 200 °C respectively. In calculating the crystallite sizes, the value of Scherrer constant K is taken as 0.94. The results indicated that the grain size of crystallite slightly increases with the increasing of reaction temperature. The small grain size of the particle is consistent with our previous discussion of size-induced red-shift of Raman spectrum. The HRTEM image is also used to investigate the shape and sizes of the crystallite. A typical HRTEM image is shown in Fig. 3b. Most of the CZTS crystallite are irregular shaped (the white-dot area) with size ranging from 5 to 20 nm. The size revealed by HRTEM is larger than the average value calculated from Debye–Scherrer equation. This difference is probably due to the wide grain size distribution of crystallite. Our current HRTEM image only revealed the crystallite with large grain size, while those in size of several nanometers were too small for its obscure boundary to be clearly observed. Therefore, statistic size of crystallite

from HRTEM is relatively larger. In spite of this, XRD and HRTEM both confirmed that the CZTS particles were composed of a large number of nanocrystals. Hence, the as-synthesized CZTS particles are referred to as nanocrystals.

3.1.2 Morphology analysis of CZTS nanocrystals

The SEM images of the as-synthesized CZTS nanocrystals are shown in Fig. 4. Samples prepared at temperature of 170 °C and above are composed of many sphere-like particles. When temperature is increased from 170 to 200 °C, the size of sphere-like particles effectively decreases from 1.5 μm to 300 nm. The morphology of particles is further supported by the HRTEM images of samples synthesized at 180 °C (sample A5). As shown in Fig. 3a, The CZTS are many gathering spherical particles with a typical diameter of 440 nm. Also, the magnified image of the spherical particle, as shown in Fig. 3b, revealed a lattice spacing of 0.32 nm, which confirmed that the sphere-like particles are kesterite structure CZTS. Samples synthesized at lower temperature of 140 and 150 °C are mostly composed of columnar rods with various diameter and length. Sphere-like particles start to appear on samples synthesized at 150 °C. When temperature increased to 160 °C, samples are composed of both column-like rods and sphere-like particles. However, column-like rods disappeared at temperature of 170 °C and above. As we have discussed in the analysis of XRD and Raman spectra, samples synthesized at temperature below 160 °C are mixtures of CZTS and impurity of sulfide, while samples synthesized at higher temperature are purely kesterite CZTS. We are reasonable to suspect that those column-like rods are related to impurity. Therefore, based on the observation of morphology, the single kesterite CZTS without secondary phase can only be obtained with reaction temperature of 170 °C and above. The above discussion revealed that not only the phase purity, but also morphology and size of as-synthesized CZTS nanocrystals are effectively influenced by the reaction temperature used in the process of microwave irradiation.

Fig. 3 a TEM image; b HRTEM image of CZTS nanocrystals prepared at 180 °C for 20 min (sample A5 or B4)



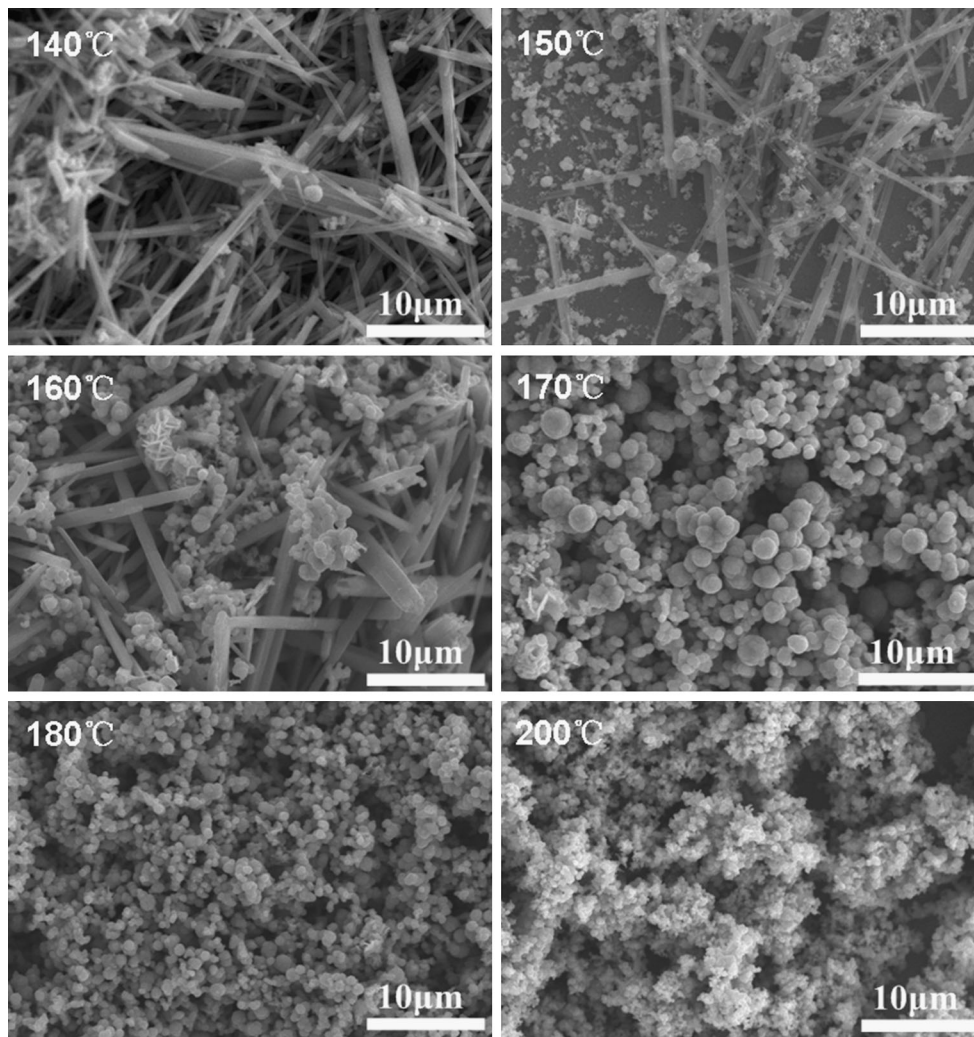
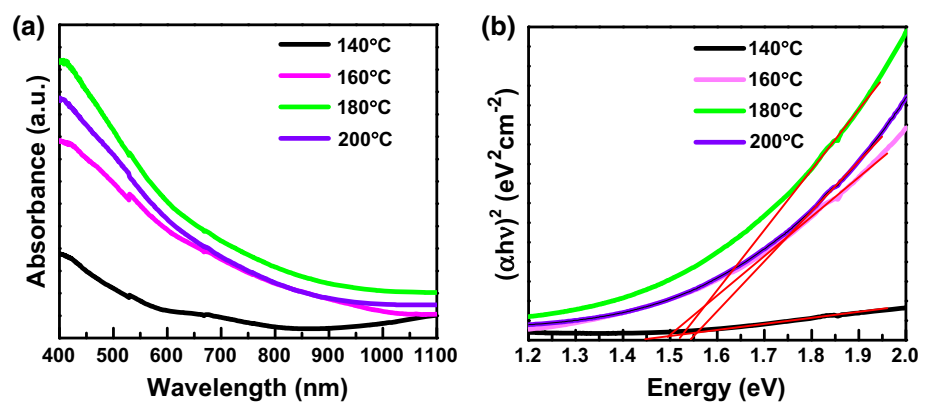


Fig. 4 SEM image of the CZTS nanocrystals prepared at different reaction temperature

Fig. 5 **a** UV–Vis absorbance spectroscopy and **b** energy band gap of CZTS nanocrystals prepared at different reaction temperature. Reaction time of all the samples was fixed to 20 min



3.1.3 Optical properties of CZTS nanocrystals

As to investigate the optical properties, CZTS thin films were prepared from CZTS nanocrystals by ink-print

method [14]. Those CZTS films were subsequently used for the measurement of UV–Vis absorption. The absorbance of CZTS nanocrystals synthesized at temperature of 140, 160, 180 and 200 °C was measured and showed in

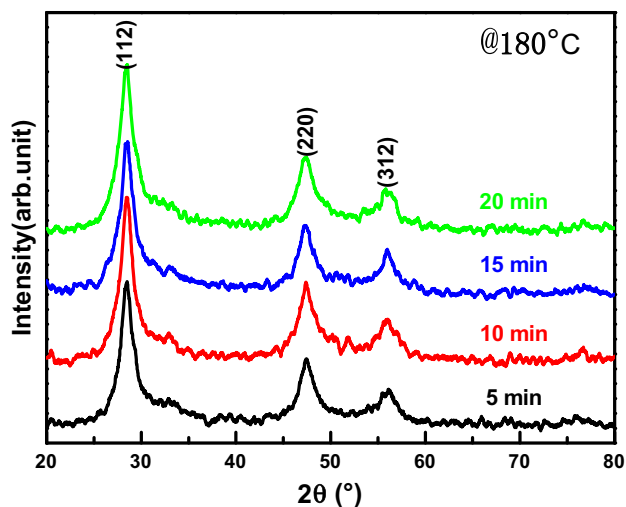


Fig. 6 X-ray diffraction patterns of the CZTS nanocrystals prepared for different reaction time. All samples were prepared at 180 °C

Fig. 5a. The optical absorption coefficient, which can be obtained by dividing the absorbance with thickness of the film, found to be larger than 10^4 cm^{-1} in visible region for all the four samples. The corresponding plots of $(\alpha h\nu)^2$ as a function of $h\nu$ was shown in Fig. 5b. Extrapolation of the linear portion of the curves to $(\alpha h\nu)^2 = 0$ gives the optical band gap E_g . The values of the optical band gap are estimated to be 1.44, 1.48, 1.52 and 1.54 eV for sample synthesized at 140, 160, 180 and 200 °C, respectively. The band gap energy increases with increasing the reaction temperature. CZTS nanocrystals synthesized at 160 °C and above are around 1.5 eV, which are appropriate for the absorption of solar spectrum. The strong absorption in the visible light region and band gap of approximately 1.5 eV is suitable to work as absorber layer of thin film solar cells.

3.2 Effect of reaction time on properties of CZTS nanocrystals

The XRD patterns of CZTS particles prepared at 180 °C for reaction time of 5, 10, 15 and 20 min were shown in Fig. 6, respectively. The major XRD diffraction peaks of all the four samples appeared at around 28.52°, 47.44° and 55.94°, can be indexed (112), (220) and (312) planes of the kesterite crystal structure (JCPDS No. 26-0575), and no obvious peaks resulting from impurities were observed. The average crystallite sizes calculated using Debye–Scherer equation based on the (112) peaks of XRD patterns are 5.67, 6.13, 5.76 and 4.97 nm for samples prepared for duration of 5, 10, 15 and 20 min, respectively.

The SEM images of the as-synthesized CZTS nanocrystalline particles are shown in Fig. 7. All the samples are composed of sphere-like particles approximately 300–500 nm in size and no obvious change of

size was observed for samples prepared for different reaction time. There are a few of column-like rods appeared in the sample synthesized at 5 min. As we have pointed out in the last section, the column-like rods are related to mixture of binary and ternary sulfide. The appearance of column-like rods is probably due to its short reaction time. Even microwave irradiation is a rapid method to obtain precise target temperature, solution heated by microwave needs approximately one or 2 min to rise from room temperature to the target 180 °C. Impurities are therefore produced during the period of temperature rising, which is an inevitable phenomenon in the process of the solution based synthesis. However, for samples synthesized for 10 min and above, the growth of CZTS is long enough to reduce the ratio of impurities in the total product and results in no appearance of column-like rods in the SEM images. The diffraction peaks of impurities were not found in the XRD patterns of samples synthesized for 5 min, which was not consistent with the SEM image. This is possible because that the sulfide produced in the solution are minority in total product whose diffraction peaks are compressed by the CZTS material. A solid explanation for this inconsistency needs a further study of the column-like rods by investigating its composition, XRD patterns, Raman spectra and HETEM image.

The analysis of XRD patterns and SEM images, along with the discussion of Raman and HRTEM in the last section, suggested that reaction time of CZTS particles with high purity kesterite phase is at least 10 min. Also, by eliminating the value of sample synthesized for 5 min, the average crystallite sizes of the CZTS nanocrystals are slightly decreases with the increasing of reaction time. Based on the above results, the synthesis of single kesterite CZTS nanocrystals by microwave irradiation method is found to be a rapid route as it requires reaction time as short as 10 min. This superiority is distinct when compared to the other solution based approaches. For example, synthesis of CZTS by solvothermal method needs 24 h [18]. Also, the synthesis using microwave irradiation is a single-step route, which is also very facile compared to the other existing approaches.

4 Conclusion

In summary, a rapid and single-step synthesis of CZTS nanocrystals using microwave-assisted solution method has been demonstrated. The influence of reaction temperature and reaction time on the phase purity, crystallographic structure, morphology and optical property of CZTS particles were investigated respectively. The CZTS particles are found to be single kesterite CZTS with no secondary phase when synthesized at reaction temperature of 170 °C

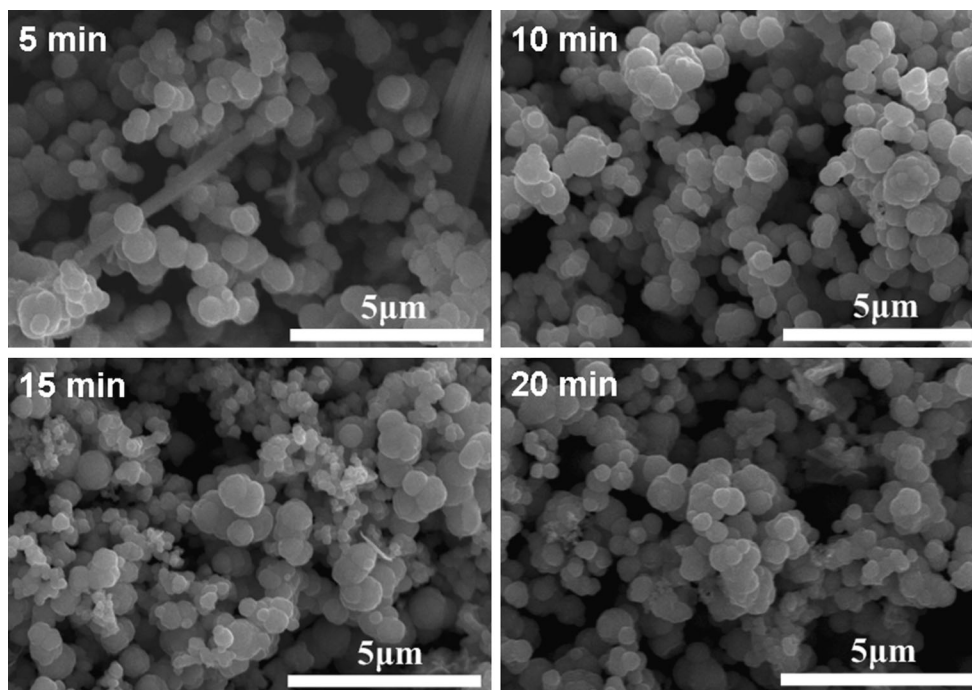


Fig. 7 SEM image of the CZTS nanocrystals prepared for different reaction time. All samples were prepared at 180 °C

and above. Each spherical CZTS particle contains many nanocrystals that are approximately 5 nm in average crystallite size. The size of sphere-like particles effectively decreases from 1.5 μm to 300 nm with increasing reaction temperature from 170 to 200 °C. The band gap energy of CZTS increases from 1.48 to 1.54 eV with increasing reaction temperature from 160 to 200 °C. The appropriate band gap makes the as-synthesized CZTS suitable to work as absorber layer of thin film solar cells. Results were also indicated that reaction time of at least 10 min is essential for the growth of single kesterite CZTS. The increasing of reaction time has no obvious influence on the morphology and size of the sphere-like CZTS particles but slightly decreases the grain size of the nanocrystals.

Acknowledgments We acknowledge the financial supports from the National Natural Science Foundation of China (Grant Nos. 51202037 and 61204049) and Science and Technology Innovation Project of Department of Education of Guangdong Province Projects (No. 2013KJCX0065).

References

1. P. Jackson, D. Hariskos, R. Wuerz, W. Wischmann, M. Powalla, *Phys. Status Solidi Rapid Res. Lett.* **8**, 219 (2014)
2. T. Wada, S. Nakamura, T. Maeda, *Prog. Photovolt. Res. Appl.* **20**, 520 (2012)
3. H. Katagiri, K. Jimbo, W.S. Maw, K. Oishi, M. Yamazaki, H. Araki et al., *Thin Solid Films* **517**, 2455 (2009)
4. D.B. Mitzi, O. Gunawan, T.K. Todorov, K.J. Wang, S. Guha, *Sol. Energy Mater. Sol. Cells* **95**, 1421 (2011)
5. X. Song, X. Ji, M. Li, W. Lin, X. Luo, H. Zhang, *Int. J. Photoenergy* **2014**, 613173 (2014)
6. W. Shockley, H.J. Queisser, *J. Appl. Phys.* **32**, 510 (1961)
7. F. Liu, Y. Li, K. Zhang, B. Wang, C. Yan, Y. Lai et al., *Sol. Energy Mater. Sol. Cells* **12**, 2431 (2010)
8. K. Moriya, K. Tanaka, H. Uchiki, *Jpn. J. Appl. Phys.* **46**, 5780 (2007)
9. T. Washio, T. Shinji, S. Tajima, *J. Mater. Chem.* **22**, 4021 (2012)
10. N.M. Shinde, R.J. Deokate, C.D. Lokhande, *J. Anal. Appl. Pyrolysis* **100**, 12 (2013)
11. K. Zhang, J. Tao, J. He, *J. Mater. Sci.: Mater. Electron.* **25**, 2703 (2014)
12. G.L. Agawane, S.W. Shin, S.A. Vanalakar, *J. Mater. Sci.: Mater. Electron.* **26**, 1900 (2015)
13. R.S. Kumar, B.D. Ryu, S. Chandramohan, J.K. Seol, S.K. Lee, C.H. Hong, *Mater. Lett.* **86**, 174 (2012)
14. W. Wang, H. Shen, F. Jiang, X. He, Z. Yue, *J. Mater. Sci.: Mater. Electron.* **24**, 1813 (2013)
15. K. Wang, P. Chen, C. Tseng, *CrystEngComm* **15**, 9863 (2013)
16. T.R. Knutson, P.J. Hanson, E.S. Aydilb, R.L. Penn, *Chem. Commun.* **50**, 5902 (2014)
17. X.T. Lu, Z.B. Zhuang, Q. Peng, Y.D. Li, *Chem. Commun.* **47**, 3141 (2011)
18. A. Wei, Z. Yan, Y. Zhao, M. Zhuang, J. Liu, *Int. J. Hydrog. Energy* **4**, 797 (2015)
19. Y.L. Zhou, W.H. Zhou, M. Li, Y.F. Du, S.X. Wu, *J. Phys. Chem. C* **115**, 19632 (2011)
20. P.R. Ghediya, T.K. Chaudhuri, *J. Mater. Sci.: Mater. Electron.* **26**, 1908 (2015)
21. S.W. Shin, J.H. Han, C.Y. Park, S. Kim, Y.C. Park, G.L. Agawane et al., *J. Alloys. Compd.* **541**, 192 (2012)
22. W. Wang, H. Shen, X. He, J. Li, *J. Nanopart. Res.* **16**, 2437 (2014)

23. J. Chen, Q. Chen, H. Yuan, T. Wang, F. Zhou, X. Dou, S. Zhuang, *J. Mater. Sci.: Mater. Electron.* **25**, 873 (2014)
24. W. Wang, H. Shen, H. Yao, *J. Mater. Sci.: Mater. Electron.* **26**, 1449 (2015)
25. Q. Guo, H.W. Hillhouse, R. Agrawal, *J. Am. Chem. Soc.* **131**, 11672 (2009)
26. P.A. Fernandes, P.M.P. Salomé, A.F. Cunha, *J. Alloys. Compd.* **509**, 7600 (2011)
27. Y. Nien, B. Zaman, J. Quyang, I. Chen, C. Hwang, K. Yu, *Mater. Lett.* **62**, 4522 (2008)
28. B. Flynn, W. Wang, C. Chang, G.S. Herman, *Phys. Status Solidi A Appl. Mater. Sci.* **209**, 2186 (2012)